An Investigation on the Effects of Different Stress Regimes on the Magnitude Distribution of Induced Seismic Events

Afshin Amini, Erik Eberhardt

Geological Engineering, University of British Columbia, Canada

Summary

An empirical study along with a series of numerical simulations is performed to investigate relationships between different stress regimes and the distribution of seismic event magnitudes arising from hydraulic fracturing activities. A database of determined focal mechanisms was compiled to determine the stress regime for different North American shale basins. Induced seismic events are identified to investigate magnitude distributions and calculate the respective b-values for each shale basin studied. In parallel, numerical modelling was performed to examine the magnitude of induced seismic events in normal, thrust, reverse and strike-slip faulting regimes. The results of this study suggest that a thrust faulting regime has a lower b-value likelihood than a strike-slip regime and therefore would be more susceptible to larger induced-seismicity events. These empirical results were reflected in the numerical results, which likewise showed that simulations modelling a thrust faulting regime generated the largest induced seismic events.

Introduction

Hydraulic fracturing is a well-established technology that is used to generate fractures and cause fracture dilation by pumping high pressure fluids into isolated borehole intervals. This serves to increase the permeability of tight oil and gas reservoir rocks and therefore increase production. Hydraulic fracturing, however, is not without secondary effects. Amongst these is the triggering of induced seismicity, which has gained attention in relation to shale gas development but also the geothermal and waste water disposal industries. In these cases, the injection of pressurized fluid can cause the effective normal stresses acting on a critically-stressed fault or persistent joint to decrease potentially leading to slip and the release of stored elastic strain energy as a seismic event. In most cases, the majority of these induced seismic events have very low magnitudes, but there have been reports of large damage-causing events. Uncertainties related to the geological environment as well as operational factors emphasize the need for targeted research. These are the subject of a large multidisciplinary research study, and reported here are results specific to the investigation of the influence of the tectonic stress regime. In this work, we first study empirical data pertaining to seismicity recorded during hydraulic fracturing operations, and analyze this data with respect to source mechanisms and magnitude distributions. This is then supplemented with a numerical modelling study using the distinct element code UDEC [1] to simulate fault slip under different stress regimes.

Empirical Study

The earthquake size distribution is known to follow a power law, the slope of which is measured as the 'b-value'. This parameter is commonly used to describe the relative occurrence of large and small events; a high b-value indicates a larger proportion of small earthquakes, and a low b-value a larger proportion of large earthquakes. Schorlemmer [2] showed that b-values vary systematically for different styles of faulting. They found that normal faulting events have the highest b-values, thrust events the lowest, and strike-slip events intermediate values. For the purpose of this study, a database was developed combining public domain stress and seismicity data with focus on several different North American shale gas basins.

First, stress data was compiled based on sources reporting focal mechanism solutions for 2996 earthquakes in the regions of interest [3–8] (Figure 1). Of note is that the database shows the stress regime for the Montney shale basin in northeastern British Columbia as being predominantly thrust faulting, and that for the Woodford shale basin in Oklahoma as being strike-slip. Data was then compiled from public disclosures of hydraulic fracturing and waste water disposal activities [9,10]. This consisted of data from 23,828 wells drilled since 2013 in northeastern B.C. and 120,247 wells drilled in the U.S. since 2009. Lastly, data was compiled from located earthquakes. This included 891 events located in northeastern B.C. after 2013 and 190,170 earthquakes recorded by the USGS across the U.S. since 2009.

Spatial and temporal filters were then applied to the database to identify induced seismic events correlated to hydraulic fracturing and waste water disposal activities. For the spatial filter, a 10 km radius was considered to take into account uncertainty in earthquake locations relative to the individual wells. The temporal filter involved a window of 3 months from the start of hydraulic injection activity to the occurrence of the earthquake. The results from this filtering are shown in Figure 2.
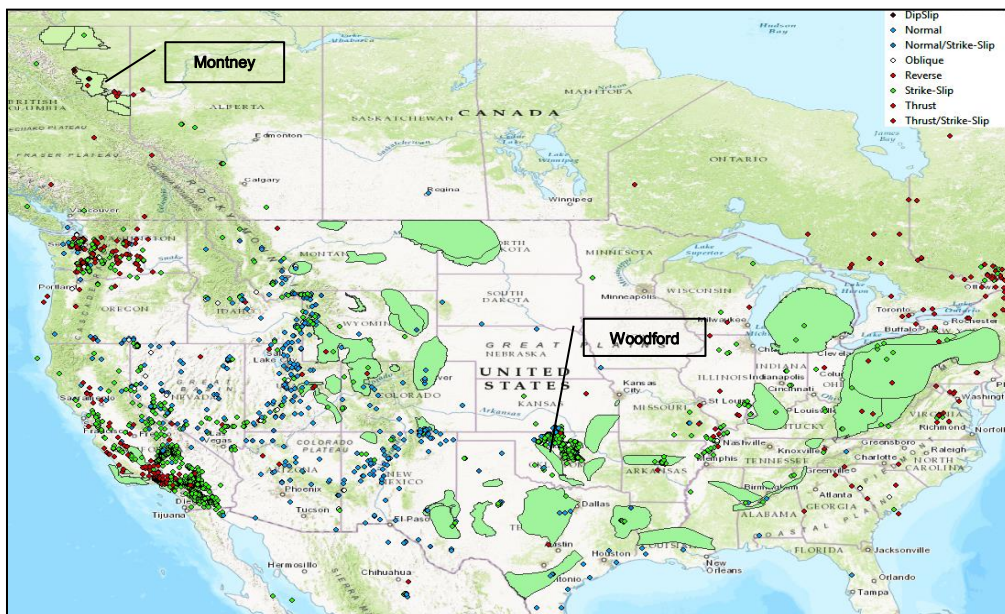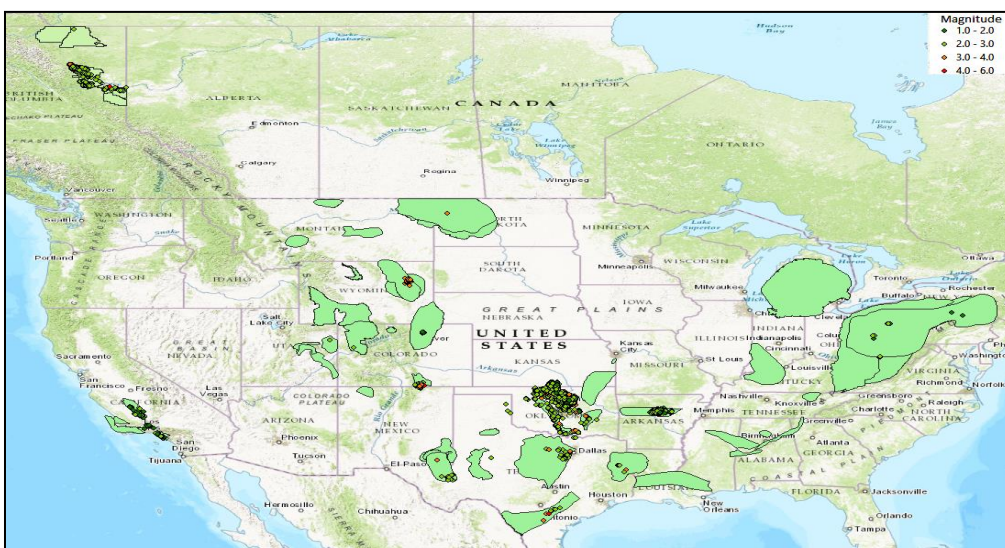

Figure 1 - Focal mechanism and shale basins

Figure 2 - Identified induced seismic events and their magnitudes

Next, comparative analyses were carried out analyzing the magnitude distributions for the different basins; reported here is that comparing the Montney and Woodford basins. After applying the filters, 363 events were identified for the Montney and 106 events were identified for the Woodford. The magnitude distributions of induced events in these basins, and respective b-values calculated using a linear regression fit, are plotted in Figure 3. The results of the empirical analysis show that the Montney basin, which represents a thrust faulting environment, shows a lower b-value of 0.99. The strike-slip environment of the Woodford basin shows a b-value of 1.49.
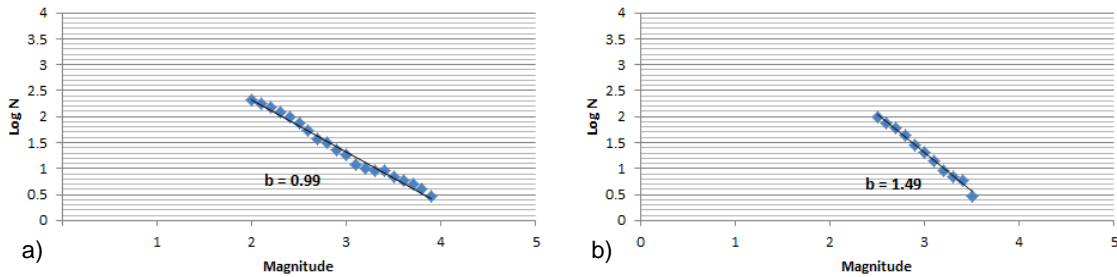

Figure 3 - Magnitude distribution and b-values for the: a) Montney and b) Woodford basins

Numerical Modeling

The effect of different stress regimes was further studied by carrying out through a series of numerical simulations using the 2-D distinct-element code UDEC^{TM} [1]. UDEC is able to model a jointed rock mass by defining an assemblage of deformable blocks bounded by a network of discontinuities of variable orientation, spacing and persistence. These discontinuities may undergo large deformations in shear and opening in response to changes in the modelled effective stresses. Zangeneh et al. [11] demonstrated that the hydro-mechanical coupling and discontinuum capabilities of UDEC makes it highly suitable for modelling hydraulic fracturing and induced seismicity.

The model geometry is shown in Figure 4. The dimensions involve a 1x1 km area, at a depth of 2500 to 3500 meters. The rock mass is modelled as an elastic material with a density of 2500 kg/m^3, and a bulk and shear modulus of 20 and 12 GPa, respectively. A critically stressed fault is located at the center of model, and extends from boundary to boundary facilitate fault propagation. This is superimposed on a network of incipient joints that represent potential fracture pathways if the injected fluid pressures exceed the rock strength (i.e. simulating a hydraulic fracture). The joint network and fault are modeled with a Coulomb slip criterion using the properties listed in Table 1. The injection depth was at 3 km with a rate of 0.4 liters per second for 10 minutes.

Joint and hydraulic properties	Incipient joints	Fault	Fault extension
Friction angle	40	30	30
Cohesion (Mpa)	10	0	10
Tensile strength (Mpa)	0.5	0	0
Residual friction angle	25	15	15
Residual Cohesion (Mpa)	0.1	0	0
Normal stiffness (Pa)	8.0E+12	8.0E+12	8.0E+12
Shear stiffness (Pa)	4.0E+10	4.0E+10	4.0E+10
jperm 1/(Pa.Sec)	83.3	83.3	83.3
azero (m)	1.0E-04	1.0E-04	1.0E-04
ares (m)	4.0E-05	4.0E-05	4.0E-05

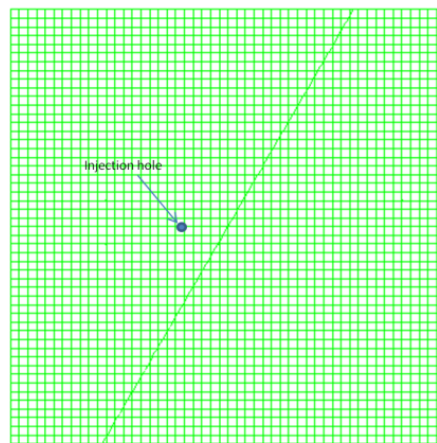Table 1 - Joint and hydraulic properties
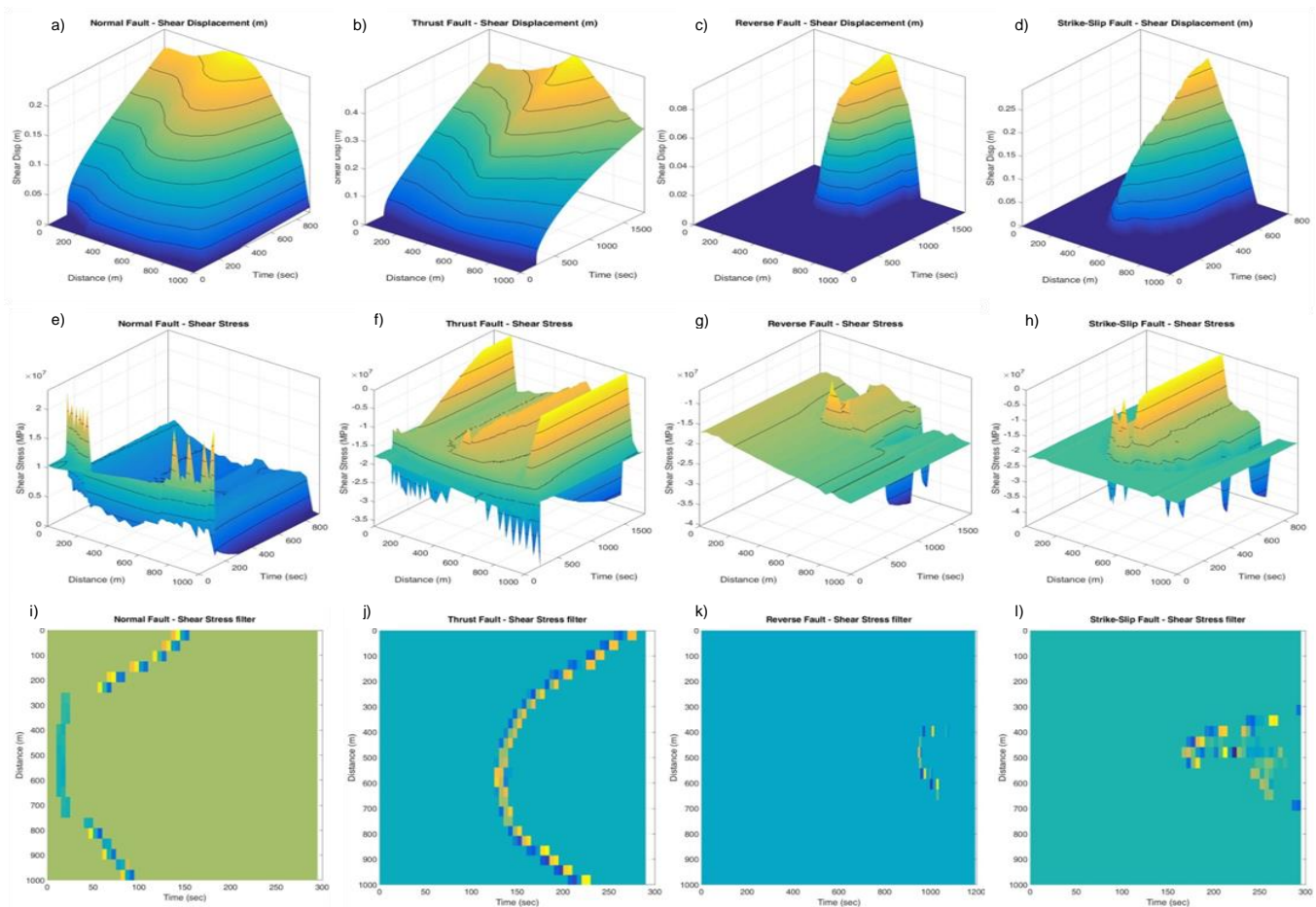

Figure 4 - 2D UDEC model (1x1 km)

Figure 5 -Numerical simulations results for Normal, Thrust, Reverse and Strike-slip faulting regimes: a-d) Shear displacement; e-h) Shear stresses (stress drop), and i-l) applied filters

The results of the simulation are shown in Figure 5. For reference, the 'Reverse' and 'Thrust' scenarios differ with respect to the fault angle (60 versus 30 degrees). Figure 5 a-d indicates that after slip initiation, the 'Normal' and 'Thrust' scenarios experience a more extensive propagation of the fault rupture. These can be compared to the stress drop, which was determined by monitoring the shear stresses along the fault as a function of injection time (Figures 5 e-h). The comparison indicates that a stress drop only occurs along a small portion of the fault interval that slipped and that the rest of the displacement is aseismic. A 1 MPa shear stress drop filter was developed based on the shear stress gradient measured along the fault, and was applied to separate seismic from aseismic fault displacements (Figure 5 i-l). Assuming the fault slip area to be circular in shape, moment magnitudes of these events were calculated based on the amount of seismic slip (i.e., slip coinciding with a stress drop, not simply the total fault slip displacement). The calculated moment magnitudes were 3.5 for the Normal stress regime, 3.2 for the Reverse regime, 3.5 for the Strike-Slip regime and 4.0 for the Thrust fault regime.

Conclusions

Results from an empirical study together with numerical modelling results were presented to investigate the effects of different stress regimes on the magnitude distribution of induced seismic events for several North American shale basins. Focus was placed on comparing the b-values for the Montney formation of northeastern B.C., which was characterized as a thrust regime, and the Woodford basin in Oklahoma, which was characterized as a strike-slip regime. The empirical and numerical analyses indicate that the magnitude distribution of events for a thrust regime are more prone to larger earthquakes than a strike slip regime, assuming the operational conditions (e.g., injection volumes, depths, etc.) are similar.

References

[1]   Itasca Consulting Group Inc. (1999). *UDEC/3DEC: Universal Distinct Element Code in 2/3 Dimensions, Version 6.0.* ICG Minneapolis.

[2]   Schorlemmer, D., Wiemer, S. and Wyss, M. (2005). Variations in earthquake-size distribution across different stress regimes. *Nature*, 437(7058): 539–542.

[3]   Heidbach, M., Rajabi, O., Reiter, M. and Ziegler, K. (2016). World Stress Map Database Release 2016. GFZ Data Services. http://doi.org/10.5880/WSM.2016.001. [Online].

[4]   Saint Luis University (2016). SLU Digital Data Focal Mechanism Page. [Online].

[5]   Snee, J-E.L. and Zoback, M.D. (2016). State of stress in Texas: Implications for induced seismicity. *Geophys. Res. Lett.*, 43: 10,208–10,214.

[6]   USGS (2016). USGS earthquake catalogue. [Online].

[7]   Kao, H., Shan, S-J., Bent, A., Woodgold, C., Rogers, G., Cassidy, J.F. and Ristau, J. (2012) Regional centroid-moment-tensor analysis for earthquakes in Canada and adjacent regions: an update. *Seismol. Res. Lett.*, 83(3): 505–515.

[8]   McNamara, D.E., Benz, H.M., Herrmann, R.B., Bergman, E.A., Earle, P., Holland, A., Baldwin, R., and Gassner, A. (2015). Earthquake hypocenters and focal mechanisms in central Oklahoma reveal a complex system of reactivated subsurface strike-slip faulting. *Geophys. Res. Lett.*, 42(8): 2742–2749.

[9]   B.C. Oil & Gas Commission (2016).,BC Oil & Gas Commission online library. [Online].

[10]   Fracfocous (2016). National hydraulic fracturing chemical registry. [Online].

[11]   Zangeneh, N., Eberhardt, E., Bustin, R.M. and Bustin, A. (2013). A numerical investigation of fault slip triggered by hydraulic fracturing. In Bunger et al. (eds.), *Effective and Sustainable Hydraulic Fracturing*. InTech Publishers, Rijeka, ISBN 978-9535111375, Chapter 23, pp. 477-488.